# High frequency spin dynamics in hybrid metallic devices

Costache, Marius Vasile

# Chapter 4

# Spin accumulation probed in multiterminal lateral all-metallic devices

We study spin accumulation in an aluminium island, in which the dc injection of a spin current and the detection of the spin accumulation are done by means of four cobalt electrodes that connect to the island through tunnel barriers. Although the four electrodes are designed as two electrode pairs of the same shape, they nonetheless all exhibit distinct switching fields. As a result the device can have several different magnetic configurations. From the measurements of the amplitude of the spin accumulation, we can identify these configurations, and using the diffusion equation for the spin imbalance, we extract the spin relaxation length $\lambda_{\rm sf} = 400 \pm 50$ nm and an interface spin current polarization $P = (10 \pm 1)\%$ at low temperature and $\lambda_{\rm sf} = 350 \pm 50$ nm, $P = (8 \pm 1)\%$ at room temperature.

## 4.1 Introduction

It is an interesting question what happens to the transport properties in non-magnetic conductors if the carriers are spin polarized. This is both a fundamental question in the field of spintronics and has also practical applications [1]. In an all-electrical setup, spin polarized carriers are injected by driving a charge current from a ferromagnet into a paramagnetic conductor. This induces an imbalance between the two spin populations, that, for diffusive systems, extends over a distance of order $\lambda_{\rm sf} = \sqrt{D\tau_{\rm sf}}$ from the interface. $\tau_{\rm sf}$ is the spin lifetime and $D$ the electron diffusion constant for the conductor. If a second ferromagnet is present within $\lambda_{\rm sf}$ from the injector, it can be used to detect the spin accumulation. In order to study spin

This chapter has been published in Physical Review B.

polarized transport in a non-magnetic metal using a lateral device, a true multi-terminal device is needed. By spatially separating the current path from the voltage probes, one can distinguish between spin accumulation and spurious interface-dependent phenomena. This technique, pioneered by Johnson and Silsbee [2], has been successfully extended to the study of spin transport in diverse systems, from metallic systems at low and room temperature [3–7] to carbon nanotubes [8], and to a lesser extent, in semiconductors [9], superconductors [10] and organic materials [11]. In the case of metallic systems, the interface between the ferromagnet and the metal has been varied from transparent to tunneling. Valenzuela et al. [12] have used a lateral spin valve device to probe the magnitude and sign of the polarization of a ferromagnet/$Al_2O_3$/Al contact as a function of the applied bias voltage.

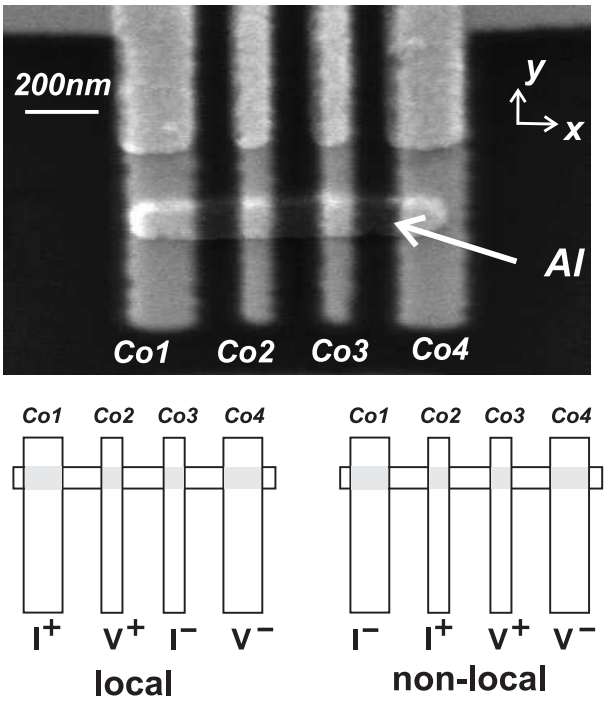


Figure 4.1: *(Top) Scanning electron microscope (SEM) image of the device. Visible are the Al island and the four Co contacts of two different widths: the wider electrodes connecting the island at its ends, have a lower switching field. (Bottom) The measurements are taken in the local and the non-local configuration. In the local measuring configuration, a current $I$ is injected from $Co1$ to $Co3$ and the voltage difference $V = V^+ - V^-$ is detected between $Co2$ and $Co4$. In the non-local measuring configuration, a current $I$ is injected from $Co2$ to $Co1$ and the voltage difference $V = V^+ - V^-$ is detected between $Co3$ and $Co4$.*

Recently, the spin accumulation in a diffusive Al island, with all lateral

dimensions smaller than $\lambda_{sf}$ has been studied [13]. The island is connected to four Co electrodes via tunnel barriers for injection/detection of the spin accumulation. However, this system suffers from several drawbacks such as difficulty of fabrication and, more importantly, large magnetic fringing fields at the end of the electrodes, which can affect the spin accumulation. Also it is not straightforward to reduce the island's volume to increase the spin accumulation.

In this work, we focus on a 1-D system (only one lateral dimension larger than $\lambda_{sf}$) in which an Al island is connected with four in-line Co electrodes, as shown in Fig. 7.15. The orientation of the electrodes' magnetization is pinned along the electrode axis in the substrate plane by the shape anisotropy and can be switched by an external magnetic field in the $\hat{\mathbf{y}}$-direction. The inner/outer electrode pairs are designed to have different widths. As the switching field is lower for the wider (outer) electrodes, we have a control on the magnetization of the individual electrodes. However, we will see that the switching fields for identically designed Co electrodes may not be the same. This is due to the small differences produced during the fabrication and to magnetic interactions between the electrodes ends. Here, we study the spin accumulation as a result of the different orientations of the four Co electrodes and we show how, from the magnitude of the spin accumulation, we can infer the magnetic configuration of the electrodes, as well as the polarization of the $Co/Al_2O_3/Al$ contacts and the spin diffusion length $\lambda_{sf}$ in Al.

## 4.2 Theoretical model

The theoretical analysis of the spin imbalance in our Al strip is based on the model for diffusive transport introduced by van Son et al. [14], Johnson and Silsbee [15] and refined by Valet and Fert [16]: there transport was analyzed for transparent ferromagnetic/non-magnetic (FM/N) interfaces. It was later understood [17–20] that the efficiency of the injection, i.e. the ratio spin polarized current to total current, can be increased by interposing a spin dependent interface between FM and N, such as a high resistance tunnel barrier.

To evaluate qualitatively the experimental results, we model the system as i) one dimensional and we assume injectors and detectors to be ii) collinear (parallel or antiparallel to $\hat{\mathbf{y}}$), and iii) point-like. Assumption i) and iii) are justified by the fact that previous measurements reported $\lambda_{sf} = 500$ nm at RT, [4, 13], larger than the island's and contacts' width, and ii) because shape anisotropy keeps the magnetization in-plane and in the direction of the contact. The contacts' positions of Co1, Co2, Co3, Co4 electrodes to the Al island are at $d_1$, $d_2$, $d_3$ and $d_4$,

with $0 \leq d_1 < d_2 < d_3 < d_4 \leq L$. We assume that a charge current $I$ is injected at $d_2$ and extracted at $d_1$. As the injectors are ferromagnetic, the injected charge current is partially spin polarized, $I_s = P_i I$, ($P < 1$ and $i = 1, 2$). This produces a space dependent spin accumulation in the Al island $\mu(x) = \tilde{\mu}(x, d_2) - \tilde{\mu}(x, d_1)$ (the minus sign because of the opposite directions of the charge current) where $\tilde{\mu} = (\mu_\uparrow - \mu_\downarrow)/2$. The spatial dependence of $\mu(x)$ in the Al strip, can be calculated by solving the 1-D spin coupled diffusion equation, Eq. 2.4, with boundary conditions $\partial\mu_{\uparrow,\downarrow}/\partial x = 0$ at either ends of the island $x = 0$ or $x = L$, that is, no charge or spin current at $x = 0, L$. The solution is given by [21]

$$\tilde{\mu}(x, d_i) = \frac{e\lambda_{\rm sf} I P_i}{2\sigma A}\Big[\exp\left(-\frac{|x - d_i|}{\lambda_{\rm sf}}\right) + C_i \exp\left(-\frac{x}{\lambda_{\rm sf}}\right) + D_i \exp\left(\frac{x - L}{\lambda_{\rm sf}}\right)\Big] \tag{4.1}$$

where $\sigma$ and A are the conductivity and sectional area of the Al strip and $C_i$ and $D_i$ are given by

$$C_i = \frac{\cosh[(L - d_i)/\lambda_{\rm sf}]}{\sinh[L/\lambda_{\rm sf}]} \quad D_i = \frac{\cosh[d_i/\lambda_{\rm sf}]}{\sinh[L/\lambda_{\rm sf}]} \tag{4.2}$$

In the limit $L \gg \lambda_{\rm sf}$, one recovers the 1-D equation [4]

$$\tilde{\mu}(x) = \frac{e\lambda_{\rm sf} I P_i}{2\sigma A} exp(\frac{-x}{\lambda_{\rm sf}}) \tag{4.3}$$

and in the limit $L \ll \lambda_{\rm sf}$, one finds the 0-D expression [13]

$$\tilde{\mu}_0 = \frac{\tau_{\rm sf} I P_i}{eN(E_F)V} = \frac{e\lambda_{\rm sf}^2 I P_i}{\sigma A L} \tag{4.4}$$

If we assume that the ferromagnetic detectors positioned at $d_3$ and $d_4$ have polarization $P_3$ and $P_4$. We measure the difference of the detectors' potentials at this points, $V(d_3) - V(d_4) = V^+ - V^-$. Then the spin dependent resistance is given by $(V^+ - V^-)/I = [P_3\mu(x = d_3) - P_4\mu(x = d_4)]/eI$. Note that in the local configuration, an Ohmic background contribution is also expected.

## 4.3 Spin valve measurements

The devices (see Fig. 7.15) are made by e-beam lithography and two-angle shadow mask evaporation process. The details on device fabrication are given in the chapter 3. The resistance of the $Al/Al_2O_3/Co$ tunnel junctions ranges from $20 - 60\ \Omega \cdot \mu m^2$, depending on the oxidation time. Measurements of the interfaces conductance with the Al in the superconducting

state revealed the possible presence of regions with high transparency at the interface, so the transport through the contacts is not entirely by tunnelling [22]. As mentioned above, the inner/outer Co electrodes have been designed to have different widths, with the outer contacts at 150 nm and the inner ones at 80 nm. This allows us to independently flip the magnetization direction of the electrodes, when an external magnetic field is slowly swept ($\approx$ 1–2 mT/second), along the contacts' direction. Nevertheless, we will present measurements in which sometimes the narrow contacts switch at lower fields than the wider ones. Measurements were performed at about 2 K and at room temperature by standard ac lock-in techniques, with a modulation frequency of 17 Hz, as describe in chapter 3. The measurements presented here are taken in the local and the non-local configuration, see Fig. 4.1. Note that due to the one-dimensional size of our Al strip, a non vanishing spin dependent signal arises even if the injectors and detectors are parallel.

### 4.3.1 Non-local spin valve configuration

In the non-local measuring configuration a current $I$ is injected from Co2 to Co1 and a voltage $V$ is detected between Co3 and Co4. Since no charge current flows through the voltage detectors, our device is not sensitive to interface or bulk magnetoresistance related effects [3], but only to the spin degree of freedom.

Figure 4.2 shows two typical non-local spin valve measurements for different devices at low temperature. The plotted signal is $(V^+ - V^-)/I$, as a function of the in-plane (in the $\hat{\mathbf{y}}$ direction) magnetic field. Referring to Figure 4.2(a) device A, at +200 mT, all contacts' magnetization are aligned parallel to the external magnetic field, in the $+\hat{\mathbf{y}}$ direction. We sweep the magnetic field toward negative values. At -80 mT, the two larger electrodes, namely Co1 and Co4, flip their magnetization (antiparallel configuration), and the detected signal increase to 90 m$\Omega$ above a zero background. Upon increasing the magnetic field further to -120 mT, the two smaller electrodes, Co2 and Co3, flip, the magnetization of the four contacts is parallel again, but now in the opposite direction ($-\hat{\mathbf{y}}$). The reverse trace show a similar behavior. Also for repeated sweeps, the field at which the magnetization switching occurs is within 20 mT of the given values. Now, what happen if all four Co electrodes switch their magnetization at different fields? Figure 4.2(b) shows such a measurement for device B. We interpret the additional steps in the signal as the fingerprint of different magnetic configurations of the electrodes. Again, at -170 mT, we start with a parallel configuration of the Co electrodes and with a background level of +70 m$\Omega$ (the nature of which is unknown). Ramping the field to positive values, at +75 mT, Co1 flips, the injectors are antiparallel and the signal increase above the

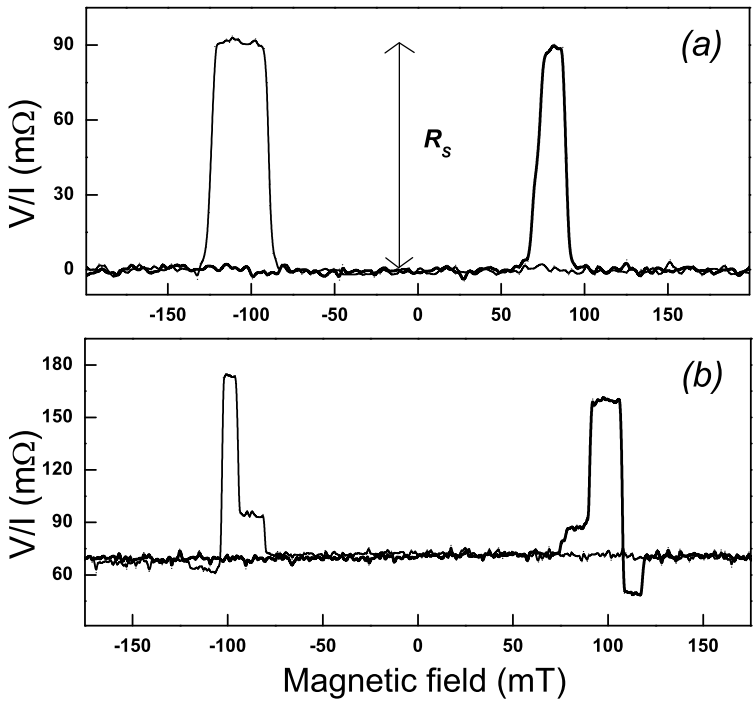


Figure 4.2: *Non-local spin valve measurement: the transresistance $V/I$ as a function of the in-plane magnetic field for positive and negative sweep direction. (a) Device A, two switch traces of the cobalt electrodes and (b) Device B, four switch traces, at low temperature (2 K).*

background level by +17 mΩ. At +90 mT the other largest electrode, Co4, reverses, so that also the detectors are antiparallel to each other. The spin signal increases now by +90 mΩ above the background level. At 106 mT, Co3 strip flips, the detectors return to parallel and the signal drops by 20 mΩ below the background level. The electrodes stay in this configuration until reaching a field of +120 mT, when the other smallest electrode, Co2, switches and the signal reaches the background level. The sweep to negative fields shows a similar behavior, with a difference in the value of the spin signal, probably due to presence of the magnetic domains in the Co strips.

It is worth mentioning at this point that, given the symmetric positions of the electrodes on the island, one cannot tell whether the electrode flipping at the lowest field, for example in Fig. 4.2(b), is Co1 or Co4. This uncertainty could have been avoided, for instance if the electrodes were arranged in a wide, narrow, wide, narrow fashion (and if the switching field is determined by the lateral dimension of the electrode only). Figure 4.3 top panel shows data for device C measured at room temperature. The behavior is similar to that of device B. The spin signal of 6-7 mΩ is smaller due to a lower spin relaxation length, and a somewhat smaller interface polarization

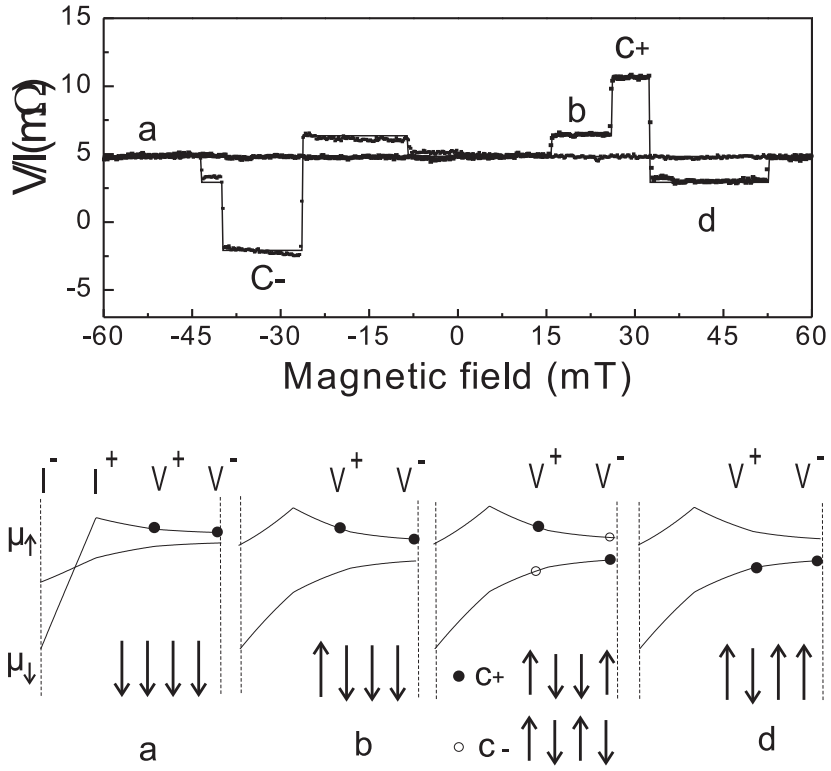


Figure 4.3: *(Top) Experimental data (dots) and fitting results (lines) using eq.1 for non-local spin valve at room temperature, device C. The letters* a *to* d *represent the different magnetic configurations as described below. (Bottom) Spatial dependence of $\mu_\uparrow$ and $\mu_\downarrow$ electrochemical potentials in the Al island for the magnetic configurations* a *to* d*, as in the top panel. The filled (open) dots indicate the potential measured by the $V^+$ and $V^-$ probes.*

at room temperature. For both positive and negative sweep directions of the magnetic field, we identify five magnetic configurations, *a*, *b*, *c+*, *c–* and *d*.

To clearly illustrate the spin contributions in different magnetic configurations, we refer to Fig. 4.3 (Bottom). Here we show schematically the spatial dependence of the spin-up ($\mu_\uparrow$) and spin-down ($\mu_\downarrow$) chemical potentials in the Al island, for the different magnetic configurations, when a charge current is injected from $I^+$ to $I^-$. $V^+$ and $V^-$ represent the position of the voltage probes. Let us assume, for the moment, the contacts to be 100% spin polarized: $V^+, V^-$ would detect either $\mu_\uparrow$ or $\mu_\downarrow$, according to the magnetization direction of the contact.

In the configuration *a* in which all contacts are parallel, and the spin related signal arises from the spatial dependence of $\mu_\downarrow(x)$.

When Co1 flips, configuration *b*, the injectors are antiparallel, a non-

uniform spin accumulation is present in the Al island, and relaxes from the points of injection, giving rise to a spin current $I_s \propto \sigma_N \cdot \nabla(\mu_\uparrow - \mu_\downarrow)$. Note that the charge current $I \propto \nabla(\mu_\uparrow + \mu_\downarrow)$ at Co3 and Co4 is absent. Although the detectors are still parallel and sensitive only to spin down channel, the signal is somewhat larger than in configuration (a), as it can be seen in the measurement, by 1.6 m$\Omega$.

When Co4 reverses, configuration *c+* (black dots), also the detectors are antiparallel, the $V^+$ electrode detects $\mu_\downarrow$ and $V^-$, $\mu_\uparrow$. In this configuration, with both injectors and detectors antiparallel to each other, we obtain the highest spin contribution, that is 6 m$\Omega$ in our measurement. When also Co3 flips, configuration *d*, the detectors now measure the spatial dependence of $\mu_\uparrow$, so that the magnitude of the signal is the same as in configuration *b* but with opposite sign. In the reverse trace, configuration *c–* (open dots) the notable difference is that Co3 flips before Co4 and the signal changes sign as $V^+$ is sensitive to spin up while $I^+$ injects spin down electrons.

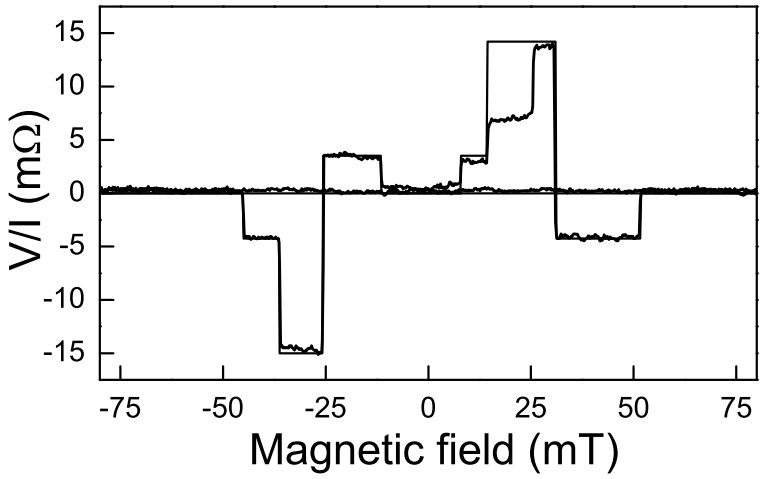


Figure 4.4: *Non-local spin accumulation at room temperature, device D. The fitting based on Eq. (4.1) returns* $\lambda_{\rm sf} = (350 \pm 50)$ *nm and a polarization of* $P = (8 \pm 1)\%$.

In the fitting of the data using Eq. 4.1, the free parameters are $|P_i| = P$ and $\lambda_{\rm sf}$, the position of the electrodes are as determined from the SEM micrographs. Also, a constant background is added to the calculated signal. We find at low temperature a spin diffusion length $\lambda_{\rm sf} = 400 \pm 50$ nm and an interface polarization $P = (10 \pm 1)\%$ and $\lambda_{\rm sf} = 350 \pm 50$ nm, $P = (8 \pm 1)\%$ at room temperature. Both these values are slightly smaller than previously found [4, 12, 13]: for the polarization, due to the nonuniform tunnel barriers in our devices [22]; for $\lambda_{\rm sf}$, probably because of the enhanced spin flip rate at the Al surface [23].

Figure 4.4 shows a non-local spin valve measurement at room tempera-

ture for device D. We observe, while sweeping at positive fields, at around +14 mT, an extra step in the signal and we interpret this as Co4 flipping its magnetization through an intermediate step. We also note in the reverse trace that Co3 reverses before Co4. Also here, the fit follows well the experimental data: this implies that all junctions have the same polarization.

### 4.3.2 Local spin valve configuration

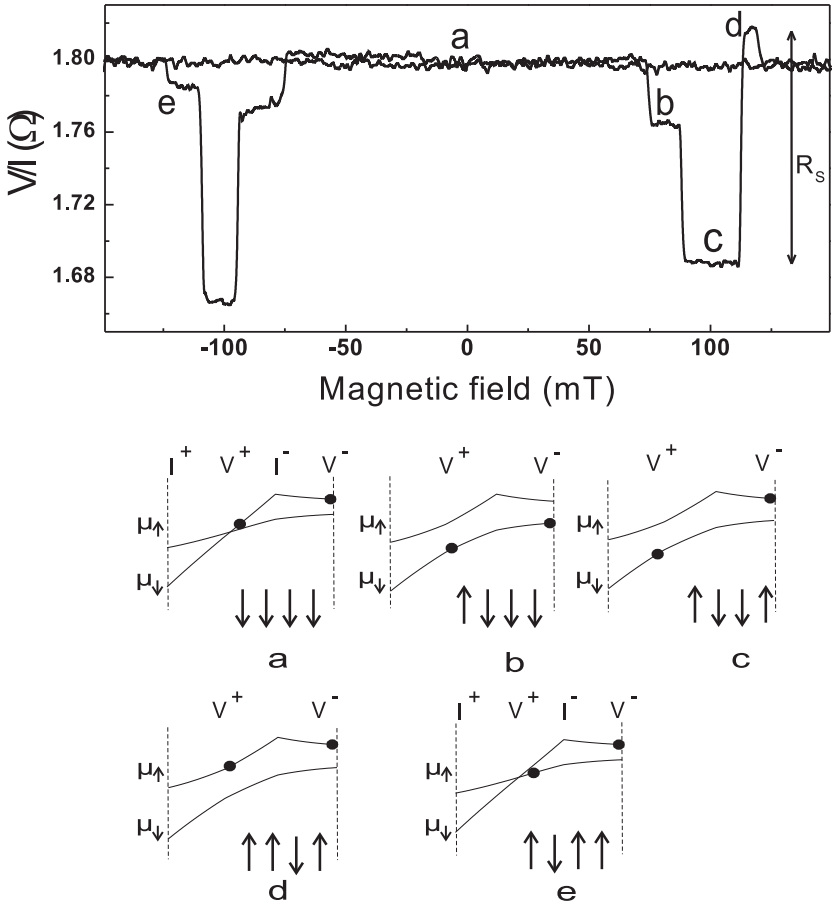


Figure 4.5: *(Top) Spin valve data in the local measuring configuration at low temperature, device E. The letters* a *to* e *represent the different magnetic configurations. (Bottom) Spatial dependence of $\mu_\uparrow$ and $\mu_\downarrow$ electrochemical potentials in the Al island for the magnetic configurations* a *to* e*, as in the top panel. The filled dots indicate the potential measured by the $V^+$ and $V^-$ probes.*

In addition, we performed spin valve measurements in the local measuring configuration. Here, a current $I$ is injected from Co1 to Co3 and a voltage $V$ is detected between Co2 and Co4. The result is shown in Fig.

4.5. A similar behavior as for non-local configuration is visible with a spin signal of 130 $m\Omega$ on the top of an Ohmic background contribution of 1.8 $\Omega$. For both positive and negative sweep directions of the magnetic field, we identify five magnetic configurations, *a*, *b*, *c*, *d* and *e*. Figure 4.5(Bottom) shows schematically the spatial dependence of the spin-up ($\mu_\uparrow$) and spin-down ($\mu_\downarrow$) chemical potentials in the Al island, for the *a*-*e* magnetic configurations. Also here, we can identify the spin contributions in these different magnetic configurations.

## 4.4 Conclusions

In summary, we have studied spin accumulation in an Al island, connected by four Co electrodes through low resistance junctions. Due to the small differences produced during the fabrication and to magnetic interactions between the Co electrodes ends, the switching fields for identically designed Co electrodes may not be the same. From the measurements of the amplitude of the spin accumulation we can identify the sequence of the magnetization switching of the ferromagnetic contacts. The analysis based on Eq. (4.1) allows us to extract $\lambda_{\rm sf}$ and $P$.

## References

[1] For recent reviews, see: D. D. Awschalom, D. Loss and N. Samarth, Semiconductor Spintronics and Quantum Computation (Springer-Verlag, 2002); I. Žutić, J. Fabian and S. Das Sarma, Rev. Mod. Phys., **76**, 3231 (2004).

[2] M. Johnson and R. H. Silsbee, Phys. Rev. Lett. **55**, 1790 (1985).

[3] F. J. Jedema, A. T. Filip, and B. J. van Wees, Nature **410**, 345 (2001).

[4] F. J. Jedema, H. B. Heersche, A. T. Filip, J. J. A. Baselmans, B. J. van Wees, Nature **416**, 713 (2002); F. J. Jedema, M. V. Costache, H. B. Heersche, J. J. A. Baselmans and B. J. van Wees, Appl. Phys. Lett. **81**, 5116 (2002).

[5] M. Urech, J. Johansson, V. Korenivski, and D. B. Haviland, J. Magn. Magn. Mater. **272**, E1469 (2004).

[6] T. Kimura, J. Hamrle, Y. Otani, K. Tsukagoshi, and Y. Aoyagi, Appl. Phys. Lett. **85**, 3501 (2004).

[7] S. Garzon, I. Žutić, and R. A. Webb, Phys. Rev. Lett. **94**, 176601 (2005).

[8] N. Tombros, S. van der Molen, and B. van Wees, Phys. Rev. B **73**, 233403 (2006).

[9] Y. Ohno, D. K. Young, B. Beschoten, F. Matsukura, H. Ohno, and D. D. Awschalom, Nature **402**, 790 (1999).

[10] D. Beckmann, H. B. Weber, and H. v. Löhneysen, Phys. Rev. Lett. **93**, 197003 (2004).

[11] V. Dediu, M. Murgia, F. C. Matacotta, C. Taliani, and S. Barbanera, Solid State Commun. **122**, 181 (2002).

[12] S. O. Valenzuela, D. J. Monsma, C. M. Marcus, V. Narayanamurti, and M. Tinkham, Phys. Rev. Lett. **94**, 196601 (2005).

[13] M. Zaffalon and B. J. van Wees, Phys. Rev. Lett. **91**, 186601 (2003).

[14] P. C. van Son, H. van Kempen, and P. Wyder, Phys. Rev. Lett. **58**, 2271 (1987).

[15] M. Johnson and R. H. Silsbee, Phys. Rev. B **37**, 5326 (1988).

[16] T. Valet and A. Fert, Phys. Rev. B **48**, 7099 (1993).

[17] A. Fert and S. Lee, Phys. Rev. B **53**, 6554 (1996).

[18] A. Filip, B. Hoving, F. Jedema, B. van Wees, B. Dutta, and S. Borghs, Phys. Rev. B **62**, 9996 (2000).

[19] G. Schmidt, D. Ferrand, L. Molenkamp, A. Filip, and B. van Wees, Phys. Rev. B **62** (2000).

[20] E.I.Rashba, Phys. Rev. B **62**, 16267 (2000).

[21] M. Zaffalon, Ph.D. thesis, University of Groningen (2006).

[22] M. Zaffalon et al., in preparation.

[23] S. O. Valenzuela and M. Tinkham, Appl. Phys. Lett. **85**, 5914 (2004).